ELSEVIER

Thermochimica Acta 266 (1995) 277–284

thermochimica acta

Melting and resolidification of $YBa_2Cu_3O_{7-x}$/silver composites ☆

Sern-Hau Lin, Nae-Lih Wu *

Chemical Engineering Department, National Taiwan University, Taipei, Taiwan

Abstract

The effects of silver and oxygen pressure on the melt-growth processing of $YBa_2Cu_3O_{7-x}$/silver (123/Ag) composite were demonstrated by employing thermal analysis and microstructural observations. As shown by DTA, Ag effectively lowers the melting, and, hence, the solidification temperatures of 123 over the entire investigated oxygen-pressure range, which is from 152 Torr (1 atm of air) down to 2 Torr. However, the melting temperature of 123 decreases while that of the excess Ag in the composite increases with decreasing oxygen pressure. This leads to a change in the solidification sequence between 123 and Ag, which, in turn, results in a significantly different Ag morphology and distribution in the melt-grown 123/Ag composites.

Keywords: Composite; Melting; Oxygen; Resolidification; Silver

1. Introduction

Significant progress in raising the critical current density (J_C) of polycrystalline $YBa_2Cu_3O_{7-x}$ (also known as the 123 compound) was achieved in several melt-growth (MG) processes [1–5]. In these processes, a bulk 123 oxide preform is first melted incongruently, then resolidified via slow cooling, and finally oxygenated at lower temperatures. A 123 bulk thus prepared typically shows the domain structure in which each domain consists of platelet-like 123 grains aligned along their *ab*-planes and Y_2BaCuO_5 (the 211 oxide) inclusions. Intra-domain J_C's in the range of, for example, 10^4–10^5 A cm^{-2} at 77K under a field up to 1 T have routinely been reported [1–5].

* Corresponding author.

☆ Dedicated to Hiroshi Suga on the Occasion of his 65th Birthday.

SSDI 0040-6031(95)02333-X

Silver has been combined with 123 oxide in many solid-state sintering processes to prepare composites which exhibit superconducting and mechanical properties superior to the pure 123 [6–14]. For example, Ag agglomerates filling the voids in a solid-state sintered 123 bulk have been found to improve resistance to thermal shock and sub-critical crack growth. In the 123/Ag composite wires and tapes, Ag provides mechanical support to the thin 123 filaments or films. Moreover, the high diffusivity of oxygen in Ag may facilitate oxygenation of a dense 123 matrix, while its high thermal conductivity helps to stabilize the superconductor when heat is generated by flux jumping. However, introduction of Ag into the MG processing methodology has been less successful than in solid-state sintering processes. Reduction in J_C due to introduction of Ag has been noted in the current atmospheric MG processes, which are conducted in 1-atm oxygen or air [15–17]. Attempts to process the wire or tape-type of 123/Ag composite by atmospheric MG processes are unsuccessful due to the expected extensive melting of Ag at their processing temperatures, ranging from 1050 to 970°C, which are well above the melting point of Ag.

We have recently demonstrated [25] that some, if not all, of the difficulties encountered in the processing of 123/Ag composites via the conventional atmospheric MG processes can be alleviated by carrying out the MG processes under greatly reduced oxygen pressures ($P(O_2) \leq 10$ Torr) at low temperatures ($920 \leq T \leq 950$°C). It was shown that bulk 123/Ag composites thus processed could contain rather uniformly distributed Ag inclusions, which are effective in reducing cracking within the 123 domains. This is in contrast to those prepared via the conventional high-temperature approach, which show preferential segregation of Ag along the 123 domain boundaries. In addition, the low $P(O_2)$ process produces 123-on-Ag tapes which exhibit c-axis preferential orientation of the 123 film normal to the Ag substrate and, particularly, minimum substrate melting.

Although there have been many reports on the phase stability of 123 oxide under sub-atmospheric oxygen pressures [18–22], much less is known for the 123/Ag composite system, except for the onset temperatures of 123 melting in the presence of Ag under oxygen pressures ranging from 1 atm to ~ 8 Torr reported by Lindemer et al. [23]. We present here the melting and resolidification characteristics, as revealed by thermal analysis and microstructural observations, of the 123/Ag composite in terms of the effects of Ag content and oxygen pressure.

2. Experimental

Differential thermal analysis (DTA) was conducted in a UVAC TGD-70000 at a constant heating or cooling rate, ranging from 0.5 to 10°C min^{-1}, under selected oxygen partial pressures. The sub-atmospheric oxygen environments were achieved either by dilution with nitrogen or by partial vacuum. Under the same oxygen pressure, these two approaches have been found to give the same DTA results. The tested samples are in powder form, consisting of 100 mg of 123 and the amounts of Ag_2O giving different 123/Ag ratios. The 123 powder was synthesized by the solid-state reaction method conducted at 930°C for several tens of hours, while the Ag_2O powder

was used as purchased. The phase purity of the 123 powder was checked by XRD and T_C measurements. In every DTA measurement, Ag_2O was found to decompose at temperatures below 400°C prior to either melting or interacting with 123 oxide at much higher temperatures ($T \geq 900$°C).

3. Results and discussion

Fig. 1 summarizes the effect of Ag addition on the melting of 123 in air. Melting of pure 123 was found to give an endothermic thermal event with the peak temperature at ~ 1027°C (curve (a)). Introduction of Ag resulted in the following additional features (curves (b)–(e)). Firstly, a peak due to melting of the Ag bulk to form Ag–O eutectic onsets at ~ 935°C. The onset temperature is invariant but the peak intensity increases with increasing Ag content. Secondly, the peak temperature due to 123 melting is shifted toward lower temperatures as the amount of Ag increases up to 10 wt% Ag_2O, after which the peak temperature became invariant with further increasing of Ag content. XRD analyses of the 123/Ag powders quenched from the 123-melting peak

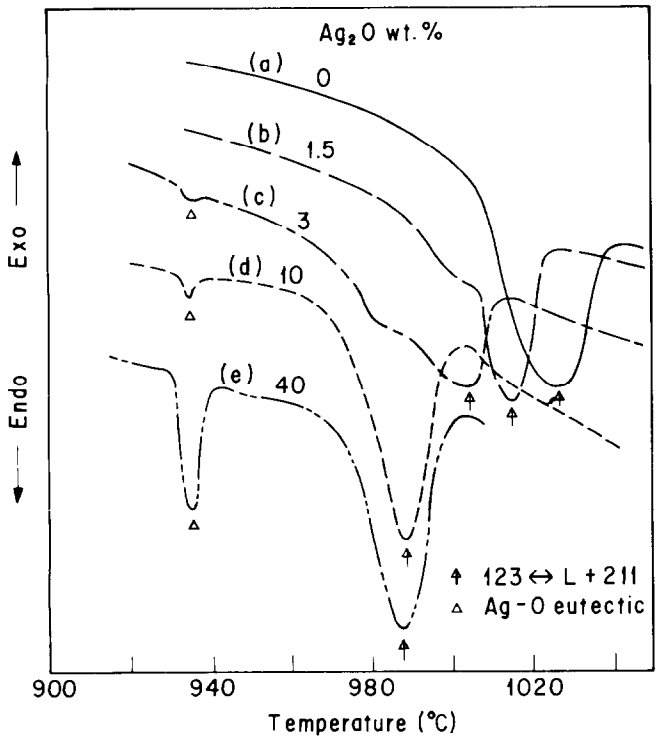

Fig. 1. Effect of Ag on the melting of 123 oxide. DTA curves of 123/Ag samples containing: (a), 0; (b), 1.5; (c), 3.0; (d), 10.0; and (e) 40.0 wt% Ag_2O, at a heating rate of 10°C min^{-1} in air.

temperatures gave, in addition to Ag, the same phases, including 123, 211, $BaCuO_2$, and CuO, as detected in the melted-and-quenched pure 123 samples. These results indicate that Ag, which is in the liquid form, helps to lower the melting temperature of 123 without producing any additonal compound and hence this reaction is simply

$$123(s) + Ag\text{–}O(l) \leftrightarrow 211(s) + Ba\text{–}Cu\text{–}Ag\text{–}O(l) + O_2 \quad (1)$$

The amount of Ag in the product liquid, according to Fig. 1, should be less than 10 wt% Ag_2O.

It was also noticed that, as shown by curves (b) and (c) in Fig. 1, for samples with low Ag contents, there often appeared a shoulder immediately in front of the 123 melting-peak maximum in the DTA spectra acquired with a heating rate of 10°C min^{-1}; this did not occur at 1°C min^{-1}. Furthermore, XRD analyses on samples quenched from these shoulder temperatures did not show the formation of any compound other than those typically resulting from melting of 123. It is possible that the appearance of these "shoulders" is due to the inhomogeneous distribution of Ag, which cause a high Ag concentration and hence a lower melting temperature of 123 locally. Indeed, these shoulder temperatures have never been lower than the 123 melting temperature of the 40 wt% sample (curve (e)), in which the Ag content is in great excess.

Peritectic melting of 123, with or without the presence of Ag, is known to be accompanied by the release of oxygen. This was evidenced by the small weight loss detected in the TG (thermal gravimetry) spectra. Accordingly, the melting temperature of 123 is expected to decrease with decreasing oxygen pressure [18–23]. For pure 123 oxide, as shown in Fig. 2, the 123 melting-peak temperature, at a heating rate of 1°C min^{-1}, was found to decrease from ~ 1015 to ~ 960°C, as $P(O_2)$ varied from 152 Torr (air) to ~ 2 Torr. For 123/Ag composites, however, the melting temperatures of 123

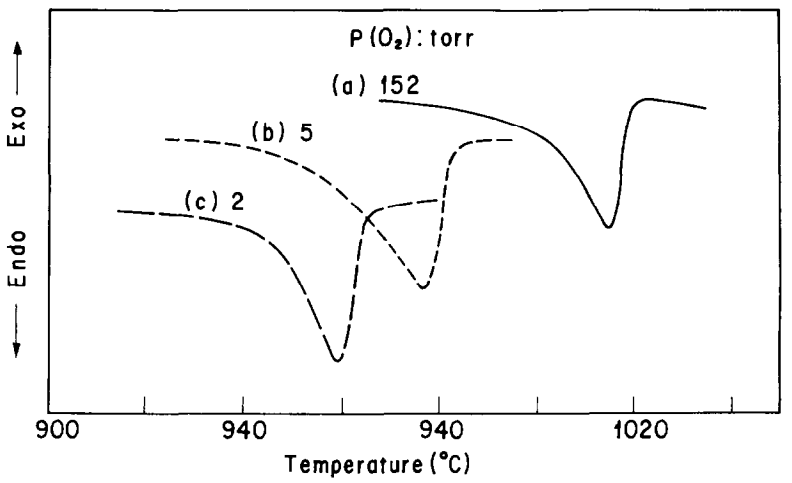

Fig. 2. Effect of oxygen pressure on the melting of 123 oxide. DTA curves of 123 samples at a heating rate of 1°C min^{-1} under an oxygen pressure, $P(O_2)$, of: (a), 152 Torr; (b), 5 Torr; and (c), 2 Torr.

and bulk Ag were found to respond to the $P(O_2)$ changes in opposite ways. As shown in Fig. 3, the peak temperature of (Ag-assisted) 123 melting decreases, while that of bulk Ag melting increases with decreasing $P(O_2)$. (A slight lowering of the Ag melting peak between $P(O_2) = 5$ and 2 Torr may be due to the alloying effect of Cu, which comes mainly from the oxide melt.) Consequently, at sufficiently low heating rates, e.g. 1°C min^{-1}, one observes these two thermal events crossing over with decreasing oxygen pressure. The curve (d) in Fig. 3 clearly demonstrates that it is possible for one to melt 123 while keeping Ag as a solid phase at low $P(O_2)$. The peak intensity of Ag melting is approximately proportional to the amount of Ag_2O, again indicating that the amount of Ag participating in the melting of 123 via reaction (1) is small.

The cooling curves of the composite samples gave two exothermic peaks due, respectively, to the solidification of Ag and 123 oxide showing the same relative positions as, but at much lower temperatures than, the endothermic melting peaks under different $P(O_2)$. In contrast to what was observed in the heating curves, the intensity of the 123 solidification peak in each cooling curve was lower than that of the Ag solidification peak, presumably due to the fact that the 123 solidification proceeds much slower than the Ag solidification. Cooling of the remaining melt gave two

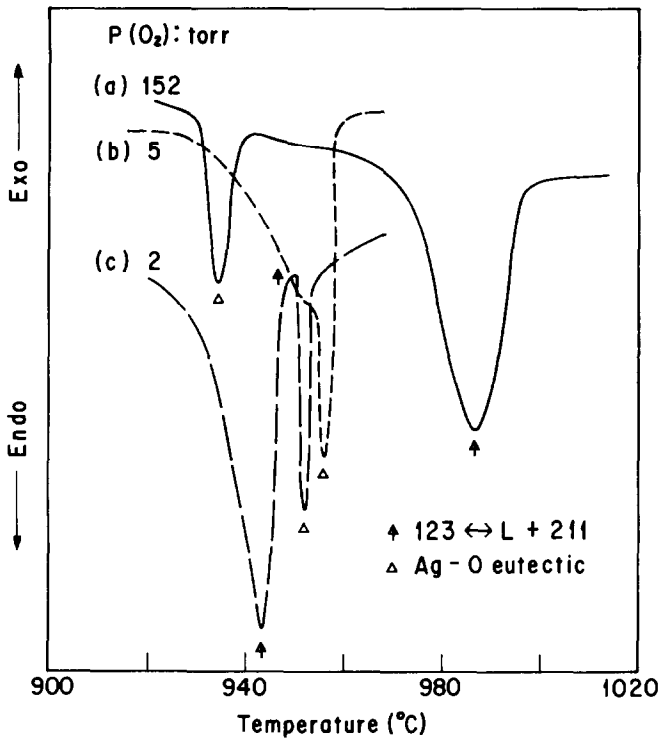

Fig. 3. Effect of oxygen pressure on the melting of 123/Ag samples containing 40 wt% Ag_2O: (a), at a heating rate of 10°C min^{-1} in air; (b), 1°C min^{-1}, $P(O_2) = 5$ Torr; and (c), 1°C min^{-1}, $P(O_2) = 2$ Torr.

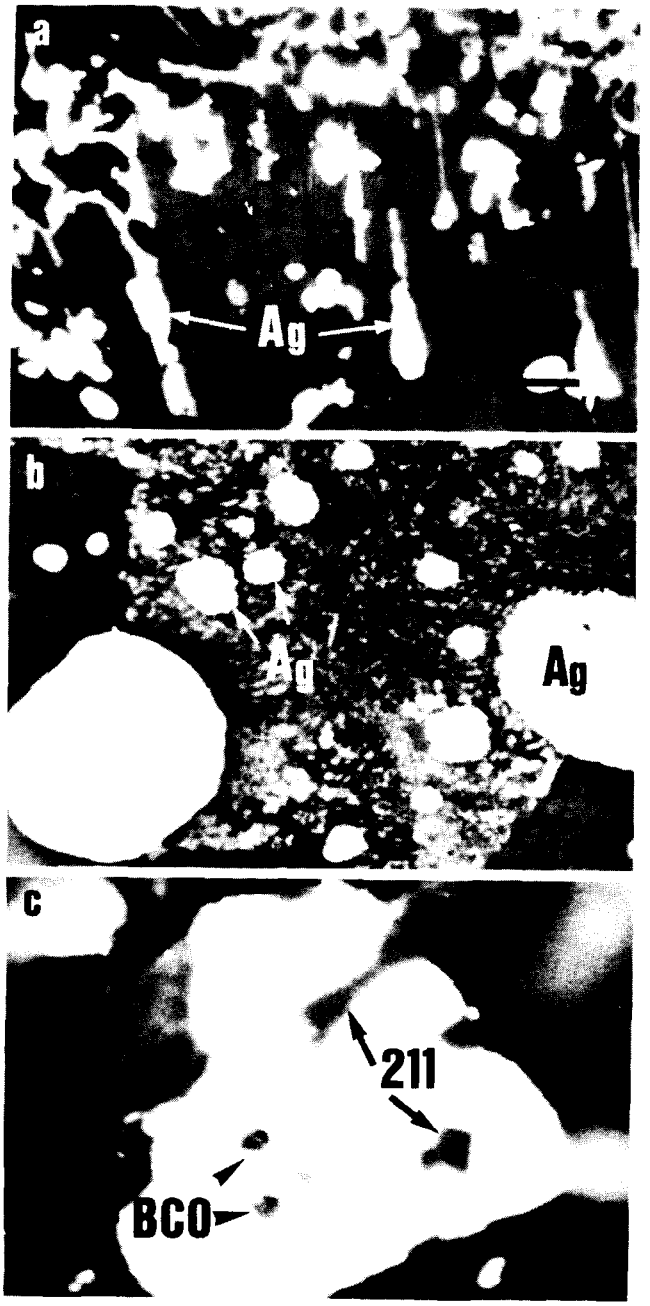

Fig. 4. Microstructures of 123/Ag composites solidified under an oxygen pressure of (a) 152 Torr; (b) 5 Torr and (c) 2 Torr (211: Y_2BaCuO_5; BCO: Ba–Cu–O).

additional endothermic peaks at temperatures below 930°C, which can be attributed to the formation of $BaCuO_2$ and CuO [24]. The difference between the melting and solidification peak temperatures decreases, and hence the extent of sub-cooling is reduced, as the cooling rate decreases. In the typical MG processes, 123 is solidified at an extremely slow cooling rate, which ranges from 1 to 5°C h^{-1}. Thus, it is concluded that the DTA heating curves, particularly those acquired at 1°C min^{-1}, serve as better guides than the cooling curves to the understanding of the MG process.

The different solidification sequences between 123 and Ag under different oxygen partial pressures were found to result in significantly varied microstructures, particularly the Ag morphology and distribution, in the solidified 123/Ag composites [25]. For example, for solidification in air, Ag remains in the liquid state throughout the major portion of the 123 solidification process (curve (a) in Fig. 3). During this period, dispersed Ag liquid appeared to be continuously pushed back by the growth fronts of 123 and eventually became "squeezed" between the growing 123 platelets or domains (Fig. 4a). The shapes of these Ag liquid agglomerates are completely random and determined mainly by the growing directions of the surrounding 123 platelets. The engulfment of Ag agglomerates into the 123 domains is accomplished as their surrounding liquid is consumed by the growth of the coherent 123 platelets in their neighborhood. However, those Ag agglomerates or particles which are originally squeezed between two 123 domains will not be engulfed into the 123 domains but remain trapped at the domain boundaries. As a result, in the composites melt-grown in air, there are fairly large amounts of Ag particles along the 123 domain boundaries and the intra-domain Ag particles exhibit rather irregular shapes.

Under $P(O_2) = 5$ Torr, Ag and 123 solidify at almost the same temperature (curve (b) in Fig. 3). Thus, the oxide melt and dispersed Ag liquid droplets are simultaneously solidified at the 123 growth front (Fig. 4b). In this case, Ag particles were engulfed one by one into the 123 domains, retaining their original geometry, which is more or less spherical, when the Ag content is less than 20 wt%. Finally, upon cooling under $P(O_2) = 2$ Torr, Ag solidifies prior to 123 (curve (c) in Fig. 3). The dispersed Ag droplets segregated during solidification and either 211 crystals or melt materials were trapped within the solidified Ag agglomerates (Fig. 4c). Furthermore, it was found that, among the three studied oxygen pressures, the extent of 123 solidification under the same cooling rate is least for $P(O_2) = 2$ Torr, presumably because solidification under this $P(O_2)$ proceeds at the lowest temperature and hence at the slowest rate.

Acknowledgement

This work is supported by the National Science Council, Republic of China under contract number NSC 84-2216-E002-020.

References

[1] S. Jin, T. Tiefel, R. Sherwood, R. van Dover, M. Davis, G. Kammlott and R. Fastnacht, Phys. Rev. B, 37 (1988) 7850.

[2] M. Murakami, M. Morita, K. Doi and K. Miyamoto, Jpn. J. Appl. Phys., 28 (1989) 1189.
[3] M. Murakami, Mod. Phys. Lett., 4 (1990) 163.
[4] M. Murakami, S. Gotoh, N. Koshizuka, S. Tanaka, T. Matsushita, S. Kanbe and K. Kitazawa, Cryogenics, 30 (1990) 390.
[5] D.F. Lee, V. Selvamanickam and K. Salama, Physica C, 202 (1992) 83.
[6] W.C. Wei and W.H. Lee, Jpn. J. Appl. Phys., 31 (1992) 1305.
[7] J.P. Singh, H.J. Leu, R.B. Poeppel, E. Van Voorhees, G.T. Goudey, K. Winsley and Donglu Shi, J. Appl. Phys., 66 (1989) 3154.
[8] J.P. Singh, J. Joo, D. Dingh, T. Warzynski and R.B. Poeppel, J. Mater. Res., 8 (1993) 1226.
[9] D.S. Kupperman, J.P. Singh, J. Faber, Jr. and R.L. Hitterman, J. Appl. Phys., 66 (1989) 3396.
[10] B. Dwir, B. Kellett, L. Mieville and D. Pavuna, J. Appl. Phys., 69 (1991) 4433.
[11] D. Shi and K.C. Goretta, Mater. Lett., 7 (1989) 428.
[12] D. Shi, Ming XU, J. G. Chen, A. Umezawa, S.G. Lanan, D. Miller and K.C. Goretta, Mater. Lett., 9 (1989) 1.
[13] M.L. Kullberg, M.T. Lanagan, W. Wu and R.B. Poeppel, Supercond. Sci. Technol., 4 (1991) 337.
[14] N.L. Wu, Y.K. Wang and S.H. Lin, CHEMTECH, (1992) 713.
[15] P. McGinn, N. Zhu, W. Chen, M. Lanagan and U. Balachandran, Physica C, 167 (1990) 343.
[16] J.A. Xia, H.T. Ren, Y. Zhao, C. Andrikidis, P.R. Munroe, H.K. Liu and S.X. Dou, Physica C, 215 (1993) 152.
[17] T. Oka, Y. Itoh, Y. Yanagi, H. Tanaka, S. Takashima, Y. Yamada and U. Mizutani, Physica C, 200 (1992) 55.
[18] T.B. Lindemer, F.A. Washburn, C.S. MacDougall, R. Feenstra and O.B. Cavin, Physica C, 178 (1991) 93.
[19] B.T. Ahn, V.Y. Lee and R. Beyers, Physica C, 162–164 (1989) 883.
[20] T. Wada, N. Suzuki, A. Ichinose, Y. Yaegashi, H. Yamauchi and S. Tanaka, Appl. Phys. Lett., 57 (1990) 81.
[21] Y. Idemoto and K. Fueki, Jpn. J. Appl. Phys., 29 (1990) 2729.
[22] G.M. Kale, Supercond. Sci. Technol., 5 (1992) 333.
[23] T.B. Lindemer, F.A. Washburn and C.S. MacDougall, Physica C, 196 (1992) 390.
[24] J. Sestak and N. Koga, Thermochim. Acta, 203 (1992) 321.
[25] N.L. Wu, H.H. Zern and C.L. Chen, Physica C, 241 (1995) 198.